Identification of the Mechanical Properties of Superconducting Windings Using the Virtual Fields Method

Jin-Hwan KIM, François NUNIO, Fabrice PIERRON and Pierre VEDRINE

Abstract— **Tensile tests were performed in order to identify the stiffness components of superconducting coils. The stereo image correlation technique was used for full-field displacement measurements. The strain components were then obtained from the measured displacement fields by numerical differentiation. Because differentiation is very sensitive to spatial noise, the displacement maps were fitted by polynomials before differentiation using a linear least-square method. Then, the four in-plane stiffnesses of the double pancake were determined using the Virtual Fields Method in the orthotropy basis.**

Index Terms— **full-field measurement, mechanical properties, superconducting coils, virtual fields method**

I. INTRODUCTION

STRONG magnetic fields induced by superconducting coils result in significant deformation of the windings. Therefore, the manufacturing of large superconducting magnets makes it necessary to determine accurately their elastic properties. Standard stiffness measurement techniques are based on homogeneous stress/strain fields in the specimens and local strain measurements through strain gauges. In the case of anisotropic materials such as superconducting windings, the number of parameters increases, so several tests need to be performed. Moreover, during the mechanical tests, such homogeneous fields are not easily obtained in superconducting windings due to their cylindrical specimen geometry. The present study aims at taking advantage of the availability of non-contact full-field measurements and inverse identification procedures in order to identify the rigidities of the Iseult 11.7 T magnet windings [1]. A very detailed FE model of the double pancake constituting the main coil of the magnet indicated that the out-of-plane displacement is significant. This implies a complex 3D behavior. In this study, a stereo image correlation technique with back-to-back cameras was chosen to observe the 3D behaviour of the double pancake. Full-field heterogeneous displacement fields were measured through the stereo image correlation technique with back-to-back cameras and then strain components were obtained from the measured displacement fields by numerical differentiation after spatial smoothing. The virtual fields method (VFM) was used as an inverse procedure to process strains for the identification of the rigidities. The virtual fields method (VFM) is based on the principle of virtual work, which describes the global equilibrium of the solid. A relevant use of the equilibrium equation leads to the identification of the constitutive parameters. In the orthotropy basis, four rigidities were determined from a single tensile test of the windings using the VFM.

II. METHODOLOGY

A. Stereo image correlation (SIC) with back-to-back cameras

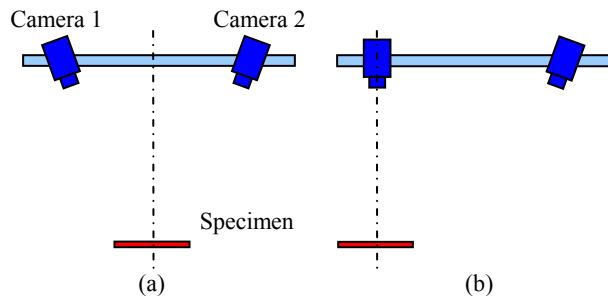The usual stereo image correlation setup is shown in Fig. 1(a).

Fig 1. Stereo image correlation set-up.

However, it was found that the usual set-up of the stereo image correlation produces slightly distorted image of the area of interest (AOI). This results in distorted strain fields and significant errors on the identified results for the rigidities. This is thought to be a problem caused by the image correlation software because of the very small strains involved, but this is still to be confirmed. In order to avoid this unexpected effect, a new camera position for the stereo image correlation was devised as shown in Fig. 1 (b). In this case, the effect of the image distortion decreased significantly.

B. The Virtual Fields Method

The principle of virtual work can be written as (if body forces are neglected):

$$-\int_V \sigma_{ij}\varepsilon_{ij}^* dV + \int_{\partial V} T_i u_i^* dS = 0 \qquad (1)$$

Jin-Hwan KIM and Fabrice PIERRON are with the LMPF research group, Arts et Métiers ParisTech, Rue Saint-Dominique, BP 508, 51000 Châlons en Champagne, France (corresponding author : +33 (0)326699186 - e-mail: jin.kim@chalons.ensam.fr, fabrice.pierron@chalons.ensam.fr).

François NUNIO and Pierre VEDRINE are with CEA, CEN de Saclay, SM/IRFU/SIS/LCAP, Bat. 123, 91191 Gif-Sur-Yvette cedex, France (e-mail: francois.nunio@cea.fr).

where V is the volume of the specimen, ∂V its boundary, σ the stress tensor, ε^* the virtual strain field, T the surface load density and u* the virtual displacement field associated to ε^*. In cylindrical coordinate system and assuming a linear elastic orthotropic behaviour, the stiffness components to be identified relate the in-plane stress to the in-plane strain components as follows:

$$\begin{pmatrix} \sigma_\theta \\ \sigma_r \\ \sigma_s \end{pmatrix} = \begin{bmatrix} Q_{\theta\theta} & Q_{\theta r} & 0 \\ Q_{\theta r} & Q_{rr} & 0 \\ 0 & 0 & Q_{ss} \end{bmatrix} \begin{pmatrix} \varepsilon_\theta \\ \varepsilon_r \\ \varepsilon_s \end{pmatrix} \quad (2)$$

where σ is the stress tensor, ε the strain tensor and the Q_{ij}'s are the stiffnesses to be determined (expressed in the orthotropy basis).

The principle of the VFM is to substitute the stress information in the above equation from the constitutive relation. Equation (1) then becomes:

$$\int_S Q_{\theta\theta}\varepsilon_\theta\varepsilon_\theta^* dS + \int_S Q_{rr}\varepsilon_r\varepsilon_r^* dS$$
$$+ \int_S Q_{\theta r}(\varepsilon_r\varepsilon_\theta^* + \varepsilon_\theta\varepsilon_r^*)dS + \int_S Q_{ss}\varepsilon_s\varepsilon_s^* dS = \frac{Fu^*(M)}{e} \quad (3)$$

where F is the applied tensile load, e the specimen thickness and $u^*(M)$ the virtual displacement of the point were the load is applied. When the material is homogeneous, the stiffness components can be moved outside of the integration sign and the choice of a particular set of virtual fields will provide a linear system relating the unknown stiffnesses to the external forces (measured by the load cell) and weighted integrals of the actual strains that can be measured from full-field measurements. The key issue of the VFM is the choice of appropriate virtual fields among the infinite possibilities. Several studies have been performed using virtual fields defined empirically. Recently, this problem has been solved efficiently with the development of the so-called special virtual fields [2] and the optimization of these special fields with respect to noise sensitivity [3].

III. RESULTS AND DISCUSSION

A. Test configuration and area of interest

In this study, the double pancake is tested according to the load configuration in Fig. 2. This test configuration yields a heterogeneous strain field at the surface of the specimen, therefore, the four rigidities can be retrieved from this single tensile test. The inner radius (R_0) of the pancake is 238.5 mm, the outer radius (R_1) 342.5 mm, and its thickness is 13 mm. Owing to the specimen size and the camera pixel aspect ratio, only a 30° angular section of the pancake specimen was investigated. The best range of the region of interest was selected as 0-30° from a finite element (FE) simulation following the selection method used in [4], so this region will be used for the rest of the study.

B. Validation on FE simulated data

In order to investigate the structural behaviour of the double pancake and validate the proposed approach, a detailed 3D FE

model was built up using the Cast3M FEA software developed by CEA. The 3D FE model is shown in Fig. 3.
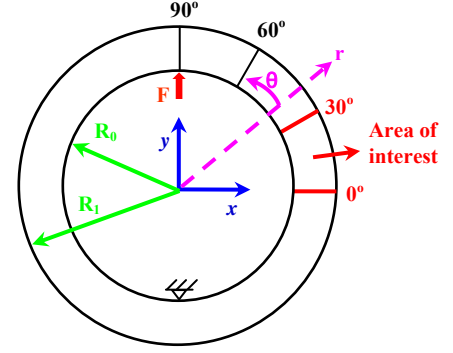

Fig 2. Geometry and test configuration of the double pancake.

The material properties used as inputs in the finite element calculations are:
Conductor (isotropic): E = 113 GPa, ν = 0.33
Insulation (transverse isotropic: 1=warp, 2=fill, 3=normal):
E_1 = 24 GPa, ν_{12} = 0.14, ν_{21} = 0.14, G_{12} = 5 GPa
E_2 = 24 GPa, ν_{13} = 0.34, ν_{31} = 0.14, G_{13} = 5 GPa
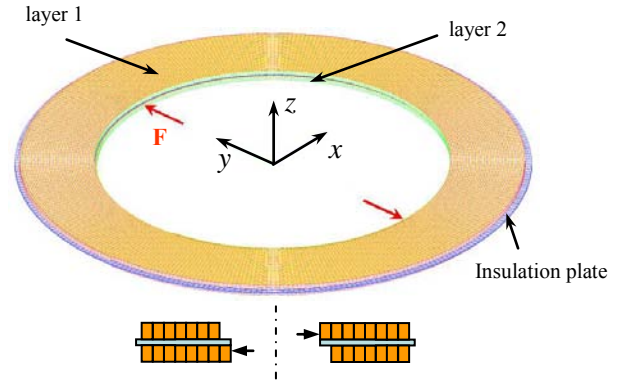E_3 = 10 GPa, ν_{23} = 0.34, ν_{32} = 0.34, G_{23} = 5 GPa

Fig 3. 3D FE model.

For the 1.5 mm insulation plate between two pancakes, the warp and fill directions are θ and r (radial) and the normal direction is z (axial). For the insulation tape between each turn of conductor, the warp and fill directions are θ and z and the normal direction is r. The applied force is 100 kN. The calculated displacement fields on the front and back surfaces of the area of interest are shown in Fig. 4 (a) and (b). As expected, the displacement is negative in the x direction and positive in the y direction. However, the out-of-plane displacement is significant. The magnitude of the out-of-plane displacements is of the same order of that of the in-plane displacements, and moreover the gradient of UZ is higher than those of UX and UY. It is considered that this peculiar behaviour of the double pancake is associated with interaction between the two layers due to the offset loading condition as shown in Fig. 3. To realistically obtain the strain fields, the differentiation process that will be used experimentally is applied. The displacement fields were smoothed using 4th order polynomial curve fitting. The strains were then obtained by analytical differentiation of these polynomials. The strain fields are presented in Fig. 5 (a)

and (b). The x strain changes from negative (compression, inner area) to positive (tension, outer area), and the y strain changes from positive (tension, inner area) to negative (compression, outer area) showing typical strain fields in a curved beam in bending. However, the shear strain is not zero in the 0° area and significant difference was observed between front and back surfaces.
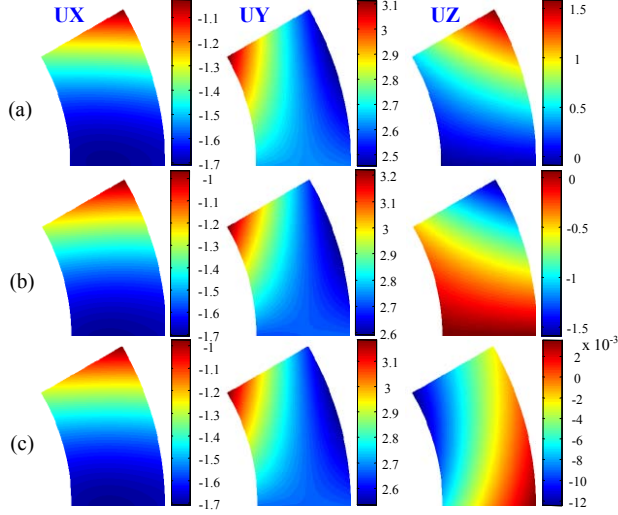

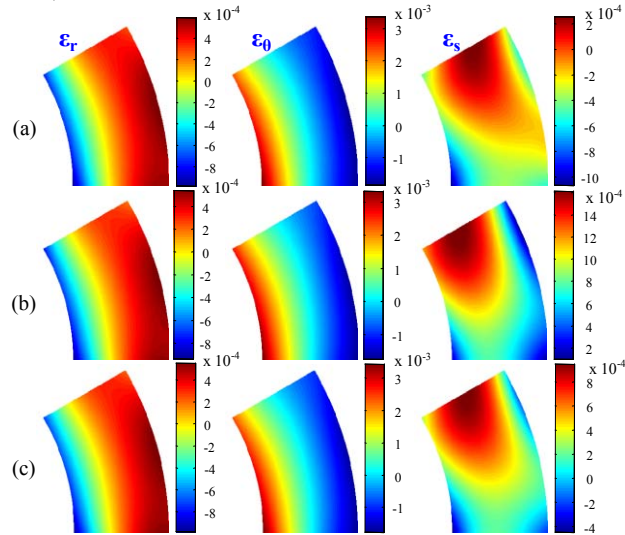Fig 4. Displacement fields from FEA (a) front face (b) back face (c) average (units: mm).

Fig 5. Strain fields from FEA (a) front face (b) back face (c) average.

The identified results of average stiffnesses of the double pancake using the VFM are shown in Table I. In this case, unexpected results were observed in the identification results. The identified results are very inconsistent between the front and back surfaces. $E_{\theta\theta}$ is considered as the stable term to identify. But the results are significantly different even between the manual and special VFM and far form the FE input (113 GPa). The identified results are negative in some cases for G_{ss}. After further investigation of the shear strain fields of both faces, it was observed that there exist high bending strains on both sides due to the specific geometrical offset configuration of the double pancake. Therefore, the average value of both

side displacements was calculated in order to get rid of the bending strain effects. The average displacement fields and the actual in-plane strain obtained from the average displacement fields are shown in Figs. 4 (c) and 5 (c). The identification results using the actual in-plane strains are shown in Table I. Interestingly, the identified results are very consistent between the manual and special VFM and the identified $E_{\theta\theta}$ is much closer to the FE input (113 GPa).

TABLE I. IDENTIFIED STIFFNESS COMPONENTS FOR THE DOUBLE PANCAKE (M: MANUAL VFM, S: SPECIAL VFM).

Rigidities		Identified values					
		front		back		average	
		M	S	M	S	M	S
E_{rr}	GPa	108.3	111.1	73.1	58.5	69.4	65.6
$E_{\theta\theta}$	GPa	172.1	139.1	70.9	85.3	100.4	100.3
$\nu_{\theta r}$		0.29	0.31	0.31	0.29	0.31	0.31
G_{ss}	GPa	18.7	-15.8	26.6	9.12	23.8	25.2

C. Experimental identification results

The initial step was to identify the material properties of the monolithic type conductor which is used for the double pancake superconducting wires. Full-field displacement fields were measured through digital image correlation (DIC). The strain fields were obtained from the displacements by numerical differentiation after spatial smoothing. Here, the diffuse approximation method [5] with r=20 was used for the smoothing. The cross section dimension of the specimen is 5.53mm x 2.78 mm. The identification was performed using the manual VFM and the identified results were: E = 92.6 GPa and ν = 0.34.

The next step was to identify the material properties of the double pancake. In the FE simulation, very complex 3D behaviour of the double pancake was observed. To get rid of the bending effects, it was decided to measure the displacement fields on both sides of the double pancake using back-to-back cameras. It should be noted here however that when the experiment was performed using a single camera for each surface, the bending effect was not cancelled out. This is due to the fact that the location of the inspected areas (front and back surfaces) is in a slightly offset position. This results in torsional effect in the strain fields. Therefore, stereo image correlation technique using two cameras for each face was finally chosen to get rid of this effect. The displacement fields on both sides of the specimen were measured and the average displacement fields were obtained. Then, the final actual in-plane strain fields were processed to identify the stiffnesses of the double pancake. The experimental implementation was performed using the stereo image correlation set-up shown in Fig. 6.

The double pancake was mounted on a tensile test machine through specially designed grips and two 2048 x 2048 pixels CCD cameras with an incidence angle observe the specimen surface. The new configuration as shown in Fig. 1 (b) was used. The displacement fields were computed from the obtained speckle pattern images using the Vic3D software. A pre-load of 1 kN was applied to avoid a settling effect before the main test.

The applied load was 9.24 kN for measurement on the front and 9.25 kN for the back face. The measured displacement fields on the front and back surfaces are shown in Fig. 7 (a) and (b).
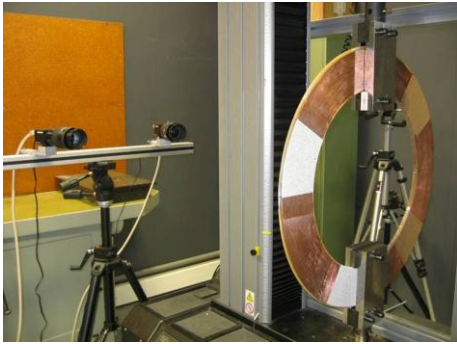

Fig 6. Stereo image correlation set-up.

The patterns of the displacement fields are very close to that from FE analysis. It is worth noting that the patterns of out-of-plane displacements and the signs are very similar between the experimental measurements and the FEA as shown in Figs. 4 and 7, though the magnitude is different due to the fixed boundary condition. But the values are significant enough to influence the results of UX and UY if a 2D technique was used. It was found that the order of UZ is 10^{-2} mm, making the correct measurements of UZ very difficult. The displacement fields were smoothed using 4th order polynomial curve fitting to obtain strain fields. The strain maps are presented in Fig. 8. ε_θ is of the order of 10^{-4} and ε_r and ε_s are of the order of 10^{-5}.
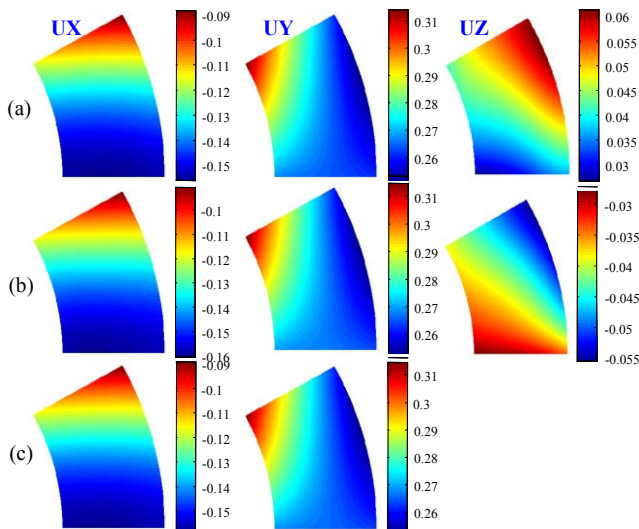

Fig 7. Displacement fields from experiment (a) front face (b) back face (c) average (units: mm).

In the same fashion, the average displacement fields (Fig. 7 (c)) were obtained from the front and back displacements and the actual in-plane strains (Fig. 8 (c)) were calculated to identify the global stiffnesses on the double pancake. The identified results are reported in Table II. As can be seen in Table II, the identified $E_{\theta\theta}$ is close to the identified longitudinal modulus of the conductor (92.6 GPa). In addition, it was observed that E_{rr} from experimental measurements is much lower than that of the simulated ones. This means that the

material properties of the insulation tape between the conductor wires used in the FEA are probably overestimated.
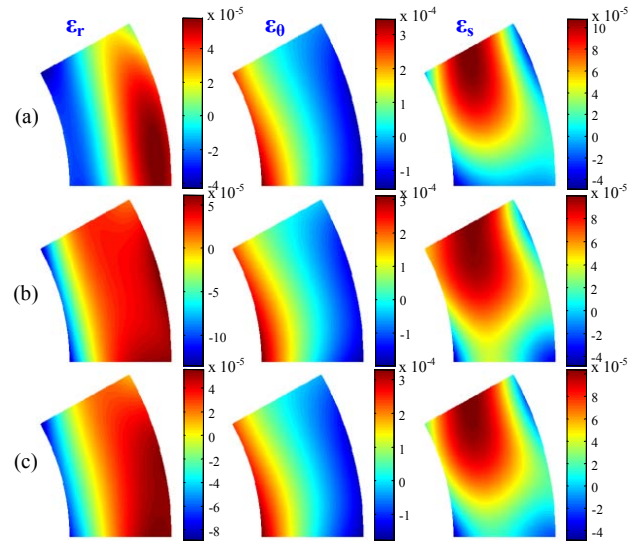

Fig 8. Strain fields from experiment (a) front face (b) back face (c) average.

TABLE II. IDENTIFIED STIFFNESS COMPONENTS FOR THE DOUBLE PANCAKE (M: MANUAL VFM, S: SPECIAL VFM).

Rigidities		Identified values					
		front		back		Back to back	
		M	S	M	S	M	S
E_{rr}	GPa	23.5	20.9	61.4	55.8	36.8	33.3
$E_{\theta\theta}$	GPa	66.4	65.8	109.7	103.8	82.9	80.6
$\nu_{\theta r}$		0.31	0.34	0.31	0.31	0.31	0.32
G_{ss}	GPa	19.6	17.2	22.7	23.6	20.9	19.6

CONCLUSION

The identified $E_{\theta\theta}$ from the double pancake is consistent with the identified longitudinal modulus of the bare conductor. The radial modulus of the pancake is lower than expected, and will be compared to an experimental compression test that will be performed on stacks of conductors.

The virtual fields method for characterizing elastic properties of double-pancakes have proven its effectiveness, and further measurements will be performed in order to study different pancake geometry and winding process.

REFERENCES

[1] P. Vedrine et al.,"Iseul/INUMAC Whole body 11.7 T MRI Magnet Status",*IEEE Trans. Appl. Supercond.*, submitted for publication.

[2] M. Grédiac, E. Toussaint, and F. Pierron, "Special virtual fields for the direct determination of material parameters with the virtual fields method. 1- Principle and definition," *International Journal of Solids and Structures*, vol. 39, no. 10, pp. 2691–2705, 2002.

[3] S. Avril, M. Grédiac, and F. Pierron, "Sensitivity of the virtual fields method to noisy data," *Computational Mechanics*, vol. 34 , no. 6, pp.439-452, 2004.

[4] R. Moulart, S. Avril, and F. Pierron, "Identification of the through-thickness rigidities of a thick laminated composite tube," *Composites: Part A*, vol. 37, pp. 326–336, 2006.

[5] S. Avril, P. Feissel, F. Pierron, and P. Villon, "Estimation of the strain field from full-field displacement noisy data: comparing finite elements global least squares and polynomial diffuse approximation," *European Journal of Computational Mechanics,* vol. 17, no. 5-7, pp. 857-868, 2008.